J|A|C|S
ARTICLES
Published on Web 01/15/2005

Reactivity and Stability of Organocopper(I), Silver(I), and Gold(I) Ate Compounds and Their Trivalent Derivatives

Waka Nakanishi, Masahiro Yamanaka,† and Eiichi Nakamura*

Contribution from the Department of Chemistry, The University of Tokyo, Hongo, Bunkyo-ku, Tokyo 113-0033, Japan and Department of Chemistry, Rikkyo University, Toshima-ku, Tokyo 171-8501, Japan

Received July 19, 2004; E-mail: nakamura@chem.s.u-tokyo.ac.jp

Abstract: Organocuprate (R_2Cu^-) reagents react with a carbon electrophile to form a new C−C bond, yet their silver and gold counterparts seldom serve for such purposes. The origin of this striking difference is discussed with the aid of the quantum mechanical calculations using hybrid density functional method. The copper reaction takes place through two steps, the nucleophilic reaction of the ate complex $R_2Cu(I)^-$ with an electrophile E^+ and the decomposition of the resulting $R_2(E)Cu(III)$ intermediate. These two steps were examined for Cu, Ag, and Au to find the reasons for the superiority of organocopper compounds to the silver and the gold counterparts. The first reaction is favored because of the higher-lying d-orbitals that directly participate in the nucleophilic reaction. The second reaction is faster with copper because of the intrinsic instability of the high valent copper species.

An organocuprate(I) reagent (e.g., R_2CuLi) and its catalytic counterpart react with an organic electrophile (E^+) such as an alkyl halide[1,2] or an α,β-unsaturated carbonyl compound[1,3] to form a new C−C bond between R and E (Scheme 1). Experimental and theoretical studies in the past decades have shown that the reactivity of the cuprate arises primarily from the high nucleophilicity of the cuprate(I) metal center of R_2Cu^- toward E^+ [4,5] and also from the instability of the resulting copper(III) intermediate $[R_2(E)Cu(III)]$[5−8] that readily undergoes reductive elimination. We have shown recently that a seemingly related organozincate(II) (R_3ZnLi) is reactive because of the high reactivity of the anionic R group rather than the d-orbital.[9,10]

Belonging to the same Group 11, however, organoargentate(I) and organoaurate(I) reagents are incomparably less useful nucleophiles in organic synthesis: We can find only a handful of examples where organoargentate[11,12] or aurate intermediates[13] are likely involved in nucleophilic C−C bond formation reactions. What could be the reason for the low nucleophilicity?

Scheme 1. Reaction of Organocuprate and Electrophile

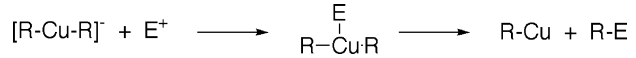

Organosilver(I) compounds are thermally too unstable to serve as a useful reagent.[14,15] Organoaurate(I) may perhaps be an intrinsically poor nucleophile, or a gold(III) intermediate may be too stable[16] to give any coupling products. Because of the paucity of actual experimental examples that we can examine for silver and gold, the question about the difference (and similarity) between cuprate, argentate, and aurate is a difficult subject to study by experiments. Having performed systematic studies on the reactivities of organocuprate(I) reagents and organocopper(III) intermediates,[17] we decided to study why argentates and aurates are inferior nucleophiles.

We made comparisons among copper, silver, and gold in two stages. First, the HOMO levels of $(CH_3)_2Cu(I)^-$, $(CH_3)_2Ag(I)^-$, and $(CH_3)_2Au(I)^-$ were examined and compared with each other, and, second, the kinetic stability of the metal(III) intermediates was examined. In this second stage, the reductive elimination reactions of $(CH_3)_3M(III)\cdot P(CH_3)_3$ and those of

† Rikkyo University.

(1) Posner, G. H. *Org. React.* **1972**, *19*, 1−113.
(2) Marshall, J. A. *Chem. Rev.* **1989**, *89*, 1503−1511.
(3) Kozlowski, J. A. *Comprehensive Organic Synthesis*; Pergamon: Oxford, 1991.
(4) Mori, S.; Nakamura, E. *Tetrahedron Lett.* **1999**, *40*, 5319−5322.
(5) Yamanaka, M.; Inagaki, A.; Nakamura, E. *J. Comput. Chem.* **2003**, *24*, 1401−1409.
(6) Nakamura, E.; Yamanaka, M.; Mori, S. *J. Am. Chem. Soc.* **2000**, *122*, 1826−1827. Dorigo, A. E.; Wanner, J.; Schleyer, P. V. R. *Angew. Chem., Int. Ed. Engl.* **1995**, *34*, 476−478.
(7) Bera, J. K.; Samuelson, A. G.; Chandrasekhar, J. *Organometallics* **1998**, *17*, 4136−4145.
(8) Stein, J.; Fackler, J. P.; Paparizos, C.; Chen, H. W. *J. Am. Chem. Soc.* **1981**, *103*, 2192−2198.
(9) Mori, S.; Hirai, A.; Nakamura, M.; Nakamura, E. *Tetrahedron* **2000**, *56*, 2805−2809.
(10) Hirai, A.; Nakamura, M.; Nakamura, E. *J. Am. Chem. Soc.* **2000**, *122*, 11791−11798.
(11) James, P. F.; O'Hair, R. A. J. *Org. Lett.* **2004**, *6*, 2761−2764. Pale, P.; Chuche, J. *Tetrahedron Lett.* **1987**, *28*, 6447−6448. Dalla, V.; Pale, P. *Tetrahedron Lett.* **1994**, *35*, 3525−3528. Dalla, V.; Pale, P. *New J. Chem.* **1999**, *23*, 803−805. Dillinger, S.; Bertus, P.; Pale, P. *Org. Lett.* **2001**, *3*, 1661−1664.
(12) Paul, A. M.; Bent, B. E. *J. Catal.* **1994**, *147*, 264−271.
(13) Hashmi, A. S. K.; Schwarz, L.; Choi, J. H.; Frost, T. M. *Angew. Chem., Int. Ed.* **2000**, *39*, 2285−2288. Ito, Y.; Sawamura, M.; Hayashi, T. *J. Am. Chem. Soc.* **1986**, *108*, 6405−6406. Togni, A.; Pastor, S. D. *J. Org. Chem.* **1990**, *55*, 1649−1664. Ito, H.; Yajima, T.; Tateiwa, J.; Hosomi, A. *Tetrahedron Lett.* **1999**, *40*, 7807−7810.
(14) Tamura, M.; Kochi, J. *Synthesis* **1971**, *6*, 303−305.
(15) Eujen, R.; Hoge, B.; Brauer, D. J. *Inorg. Chem.* **1997**, *36*, 3160−3166.
(16) Komiya, S.; Albright, T. A.; Hoffmann, R.; Kochi, J. K. *J. Am. Chem. Soc.* **1977**, *99*, 8440−8447. Komiya, S.; Ochiai, S.; Ishizaki, Y. *Inorg. Chem.* **1992**, *31*, 3168−3169.
(17) Nakamura, E.; Mori, S. *Angew. Chem., Int. Ed.* **2000**, *39*, 3751−3771.

10.1021/ja045659+ CCC: $30.25

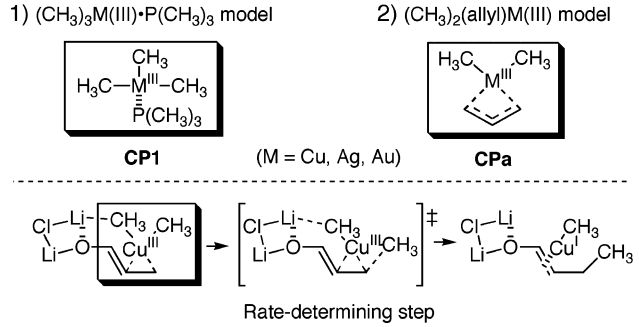

Figure 1. $(CH_3)_3M(III)\cdot P(CH_3)_3$ and $(CH_3)_2(allyl)M(III)$ (M = Cu, Ag, and Au) as models of the reductive elimination stage in the conjugate addition.

$(CH_3)_2(allyl)M(III)$ were compared for the three metals. The analyses at both stages indicated that the copper reagent is better suited for nucleophilic reactions than the silver or gold reagents.

Chemical Models

1. $(CH_3)_2M^-$ Models. We previously compared the nucleophilic reactivity of organocopper ($CH_3Cu(I)$, $(CH_3)_2Cu(I)^-$) and zinc reagents ($(CH_3)_2Zn(II)$, $(CH_3)_3Zn(II)^-$) through comparison of their HOMO energy level.[9] Similarly, we take here the HOMO energy levels of $(CH_3)_2Cu(I)^-$, $(CH_3)_2Ag(I)^-$, and $(CH_3)_2Au(I)^-$ as a measure of their relative nucleophilicity. The copper, silver, and gold series are denoted with subscripts, **c**, **s,** and **g**, respectively, such as **TSc** (transition structure for copper).

2. Decomposition of M(III) Intermediates. The ground design of the present study is based on the basic mechanistic framework of the conjugate addition of $(CH_3)_2CuLi$ to an α,β-unsaturated carbonyl compound that we proposed recently (Figure 1).[18]

(1) Decomposition of $(CH_3)_3M(III)\cdot P(CH_3)_3$ Intermediates. $(CH_3)_3Cu(III)\cdot P(CH_3)_3$ provides important information on the properties of the higher oxidation state of copper.[6,19,20] We therefore compared first the Cu, Ag, and Au intermediates, $(CH_3)_3M(III)\cdot P(CH_3)_3$, with each other.

(2) Decomposition of $(CH_3)_2(allyl)M(III)$ Intermediate. In our recent work, we studied $(CH_3)_2(allyl)Cu(III)$ intermediate as a model, more advanced than $(CH_3)_3M(III)\cdot P(CH_3)_3$ of the conjugate addition and the allylation reactions of the $(CH_3)_2CuLi$ reagent.[18,21] The study provided information unavailable from the simpler $(CH_3)_3Cu(III)$ model study. We therefore performed equivalent studies on Ag and Au. The same trend as the one found for $(CH_3)_3M(III)$ was found.

We did not perform any further analysis of more realistic reactions such as conjugate addition and alkylation reactions of organoargentate and organoaurate reagents, since these reactions do not take place in actual experiments.

Computational Methods

All calculations were performed with a GAUSSIAN 98 package.[22] The geometry optimization was performed at the B3LYP[23] level with the basis set denoted as 631SDD consisting of the SDD basis set including a double-ζ valence basis set[24] with the Stuttgart's quasi-relativistic effective core potential for Cu,[25] Ag,[26] and Au[26] and the 6-31G(d) sets[27] for others. The SDD basis set used here is a slightly different version of the one used in our copper-specific studies[5,18] but gave structures and energetics for copper almost identical with those in the previous studies.[18] The natural charges were calculated by the natural population analysis at the same level as the one used for geometry optimization.[28] The B3LYP/631SDD level calculation shows good agreement with the experimental data for organogold[29] and also shows almost identical results for the organocopper to the one we reported.[18] The organosilver and organogold complexes reproduce the X-ray crystallographic data very well (see Supporting Information).[8,15,30] All stationary points were adequately characterized by normal coordinate analysis. Gibbs free energies were obtained on the basis of the calculated frequencies.[31] Energies are shown in kcal/mol and bond lengths in Å. Kohn−Sham orbitals[32] were obtained for MO analysis.

Results and Discussions

1. $(CH_3)_2M(I)^-$ Models. In our previous work shown in the left part of Figure 2,[4] a Kohn−Sham MO analysis of the bent and liner structures of $(CH_3)_2Cu(I)^-$ was performed. In the linear conformer of $(CH_3)_2Cu(I)^-$ which is a global minimum (D_{3h} symmetry, Figure 2a), the HOMO represents the copper s+d_z2 orbital, and the carbons s+p orbitals lie just below this HOMO. The HOMO of the linear conformer is suitable for interaction with σ^*-orbital and hence responsible for the S_N2-reaction with an alkyl halide. Bending of the C−Cu−C array under C_{2v} symmetry pushes up the d_{xz} orbitals of the copper atom to mix it with the s+p orbitals of carbon atom (Figure 2 top left box), and the symmetry of this new HOMO is suitable for back-donative interaction with the π^* orbital of an electron-deficient olefin. The energy loss due to the bending (e.g., examined with 112° for Cu, Ag, and Au; 25.3, 24.8, 35.9 kcal/mol, respectively) is compensated by the energy gain from the d−π^* back-donation. Therefore, the level of the d_z2 orbital (a_1'-HOMO; responsible in an alkylation reaction) and the difference of the energy level between a_2'' HOMO-1 and e'' HOMO-2 (responsible in a conjugate addition) are the parameters critical for the evaluation of the organocuprate(I) species.[4]

The very low levels of a_1'-HOMOs of $(CH_3)_2Ag(I)^-$ and $(CH_3)_2Au(I)^-$ (Figure 2b,c) immediately suggest that these compounds must be much less nucleophilic than $(CH_3)_2Cu(I)^-$,

(18) Yamanaka, M.; Kato, S.; Nakamura, E. *J. Am. Chem. Soc.* **2004**, *126*, 6287−6293.
(19) Snyder, J. P. *J. Am. Chem. Soc.* **1995**, *117*, 11025−11026.
(20) Snyder, J. P. *Angew. Chem., Int. Ed. Engl.* **1995**, *34*, 80−81.
(21) Nakamura, E.; Mori, S.; Morokuma, K. *J. Am. Chem. Soc.* **1997**, *119*, 4900−4910. Mori, S.; Nakamura, E. *Chem. Eur. J.* **1999**, *5*, 1534−1543.
(22) Frisch, M. J.; Trucks, G. W.; Schlegel, H. B.; Scuseria, G. E.; Robb, M. A.; Cheeseman, J. R.; Zakrzewski, V. G.; Montogomery, J. A., Jr.; Stratmann, R. E.; Burant, J. C.; Dapprich, S.; Millam, J. M.; Daniels, A. D.; Kudin, K. N.; Strain, M. C.; Farkas, O.; Tomasi, J.; Barone, V.; Cossi, M.; Cammi, R.; Mennucci, B.; Pomelli, C.; Adamo, C.; Clifford, S.; Ochterski, J.; Petersson, G. A.; Ayala, P. Y.; Cui, Q.; Morokuma, K.; Malick, D. K.; Rabuck, A. D.; Raghavachari, K.; Foresman, J. B.; Cioslowski, J.; Ortiz, J. V.; Stefanov, B. B.; Liu, G.; Liashenko, A.; Piskorz, P.; Komaromi, I.; Gomperts, R.; Martin, R. L.; Fox, D. J.; Keith, T.; Al-Laham, M. A.; Peng, C. Y.; Nanayakkara, A.; Gonzalez, C.; Challacombe, M.; Gill, P. M. W.; Johnson, B. G.; Chen, W.; Wong, M. W.; Andres, J. L.; Head-Gordon, M.; Replogle, E. S.; Pople, J. A. *Gaussian 98*, revision A.6; Gaussian, Inc.: Pittsburgh, PA, 1998.
(23) Becke, A. D. *J. Chem. Phys.* **1993**, *98*, 5648−5652. Lee, C. T.; Yang, W. T.; Parr, R. G. *Phys. Rev. B* **1988**, *37*, 785−789.
(24) Dunning, T. H.; Hay, P. J. *Modern Theoretical Chemistry*; Plenum: New York, 1976; Vol. 3.
(25) Dolg, M.; Wedig, U.; Stoll, H.; Preuss, H. *J. Chem. Phys.* **1987**, *86*, 866−872.
(26) Andrae, D.; Haussermann, U.; Dolg, M.; Stoll, H.; Preuss, H. *Theor. Chim. Acta* **1990**, *77*, 123−141.
(27) Hehre, W. J.; Radom, L.; Schleyer, P. v. R.; Pople, J. A.; *Ab Initio Molecular Orbital Theory*; John Wiley & Sons: New York, 1986. References cited therein.
(28) Reed, A. E.; Weinstock, R. B.; Weinhold, F. *J. Chem. Phys.* **1985**, *83*, 735−746.
(29) Zhao, J. Y.; Zhang, Y.; Zhu, L. G. *J. Mol. Struct.* **2004**, *671*, 179−187.
(30) Zhu, D. M.; Lindeman, S. V.; Kochi, J. K. *Organometallics* **1999**, *18*, 2241−2248.
(31) Scott, A. P.; Radom, L. *J. Phys. Chem.* **1996**, *100*, 16502−16513.
(32) Kohn, W.; Sham, L. *Phys. Rev.* **1965**, *140*, A1133−1138.

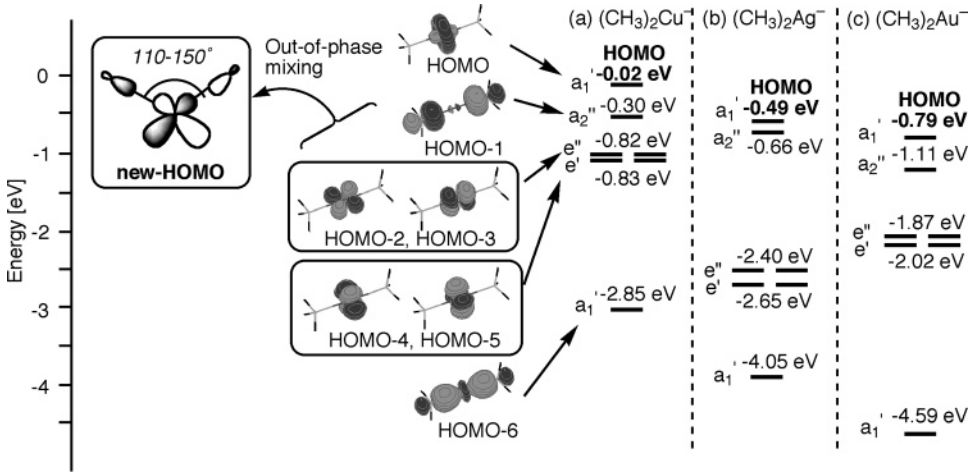

Figure 2. Some high-lying Kohn−Sham orbitals of $(CH_3)_2M(I)^-$ (M = Cu (a); Ag (b); Au (c)).

Scheme 2. Chemical Models of Reductive Elimination of the $(CH_3)_3M(III)\cdot P(CH_3)_3$ Complexes (M = Cu, Ag, and Au)

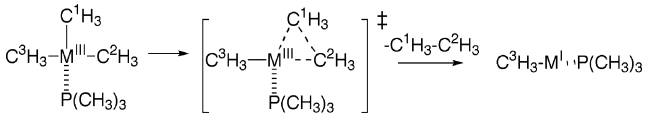

especially in the alkylation reaction. In addition, a_2'' HOMO-1 (methyl anion) and e'' HOMO-2 (d_{xz}) of $(CH_3)_2Ag(I)^-$ are much separated energetically from each other and will hardly mix together, a feature necessary for the conjugate addition reaction.[4] The energy difference between a_2'' HOMO-1 and e'' HOMO-2 of $(CH_3)_2Au(I)^-$ is smaller but is still larger than those of $(CH_3)_2Cu(I)^-$. Given the wider gaps and the lower energy levels of the d orbitals, $(CH_3)_2Ag(I)^-$ and $(CH_3)_2Au(I)^-$ should be less nucleophilic than $(CH_3)_2Cu(I)^-$.

2. Decomposition of M(III) Intermediates. 2.1. Reductive Elimination of Triorganometal(III)·phosphine $(CH_3)_3M(III)\cdot P(CH_3)_3$. The model reaction of the reductive elimination of $(CH_3)_3M(III)\cdot P(CH_3)_3$ (M = Cu, Ag, and Au) is shown in Scheme 2. The reaction begins with a tetracoordinated complex (**CP1**) which then goes to a tetracoordinated TS (**TS1**) and ends with the ethane and $(CH_3)M(I)\cdot P(CH_3)_3$ (**PD1**).

Potential and Gibbs Free Energy Profiles of the Reaction Path. Potential and Gibbs free energies of the reductive elimination of the $(CH_3)_3M(III)\cdot P(CH_3)_3$ complexes were calculated for the structure optimized at the B3LYP/631SDD level and are shown in Figure 3. The TS potential energy (and Gibbs free energy) for reductive elimination of organocopper is +17.7 (+16.1) kcal/mol; organosilver, +24.9 (+20.6) kcal/mol; and organogold, +35.0 (+31.1) kcal/mol. Taken together with the HOMO data in the previous section, the cuprate(I) is expected to be more reactive than the argentate(I) and aurate(I) in the stage of both the formation and the decomposition of the $R_2(E)M(III)$ intermediates.

The Structures of Triorganometal(III)·Phosphine $(CH_3)_3M(III)\cdot P(CH_3)_3$. To probe the reactivity of the $(CH_3)_3M(III)$ complexes, we examine the structures of the complexes and the TSs (Figures 4 and 5, respectively). While the structures of the $(CH_3)_3M(III)\cdot P(CH_3)_3$ are similar to each other, the TSs are not: **TS1s** and **TS1g** are significantly different from **TS1c**. While the metal in **TS1c** is tetracoordinated (i.e., $(CH_3)_3Cu(III)$ moiety is in a "distorted T-shape"), those in **TS1g**

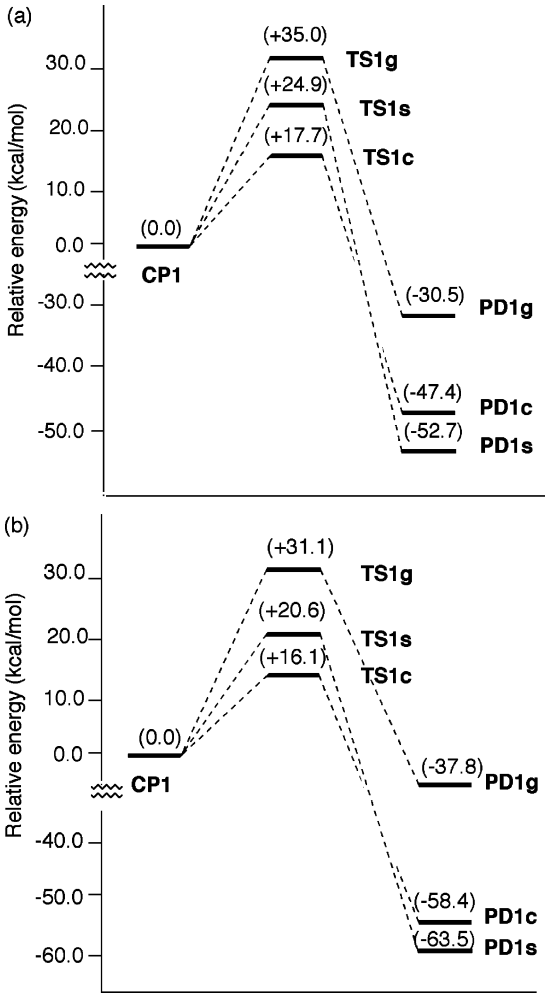

Figure 3. (a) Potential and (b) Gibbs free energy profiles of reductive elimination of $(CH_3)_3M(III)\cdot P(CH_3)_3$ (M = Cu, Ag, and Au) at the B3LYP/631SDD level.

and **TS1s** has lost the $P(CH_3)_3$ ligand and is in a "Y-shape" (Au−P: 4.588 Å; Ag−P: 3.973 Å).

Reductive Elimination of Triorganometal(III) $(CH_3)_3M(III)$. In light of these dissociative pathways of reductive elimination for silver and gold, we also examined reductive elimination of $(CH_3)_3M(III)$ by itself (Scheme 3). Free $(CH_3)_3Cu(III)$ without the ligand coordination does not exist as

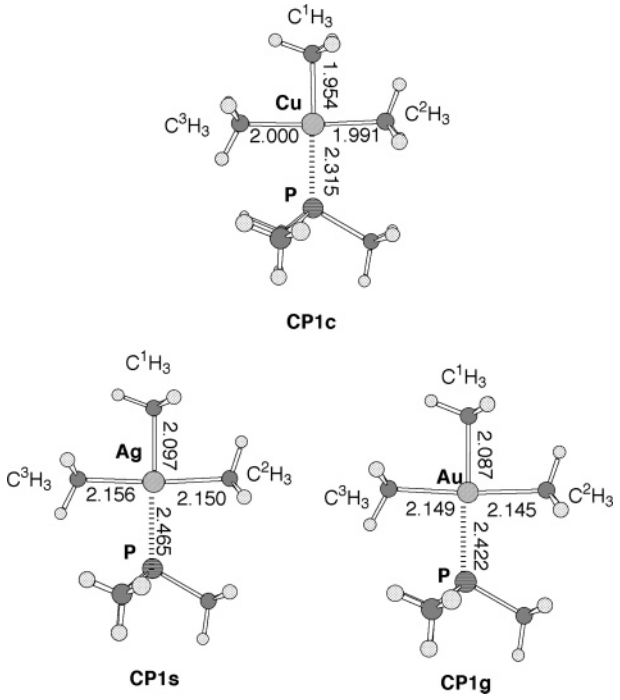

Figure 4. 3D structures of $(CH_3)_3M(III)\cdot P(CH_3)_3$ (M = Cu, Ag, and Au) (**CP1**) at the B3LYP/631SDD level. Numbers refer to bond lengths (Å).

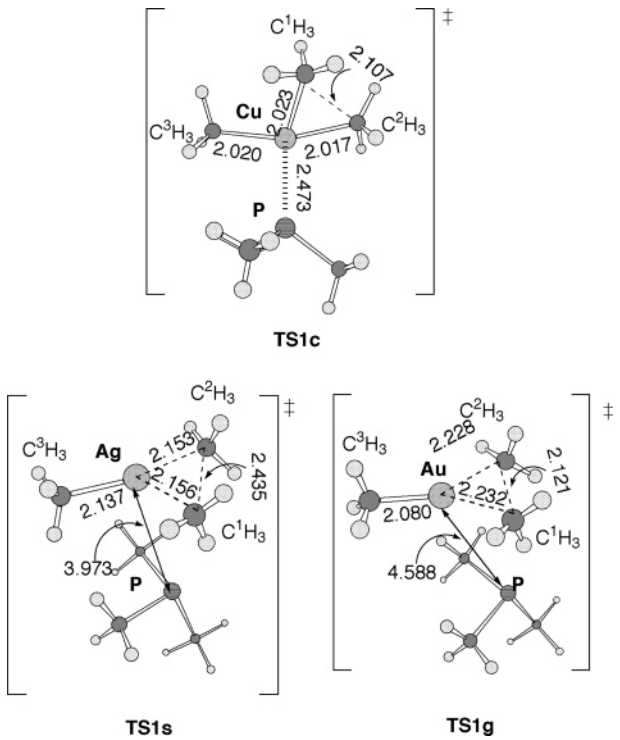

Figure 5. TSs of $(CH_3)_3M(III)\cdot P(CH_3)_3$ (M = Cu, Ag, and Au) (**TS1**) at the B3LYP/631SDD level. Numbers refer to bond lengths (Å). The C^1-M-C^2 angles (M = Cu, Ag, and Au) are 63.2°, 68.8°, and 56.8°, respectively.

a stable compound and therefore was not studied.[5,6,19] The energetics for organosilver and gold are shown in Supporting Information and cited in Table 1. The activation energies for the reductive elimination of **CP1** ($\Delta E_1^{\ddagger}$) and for the reductive elimination of **CP1** via **CP2** ($\Delta E_2^{\ddagger}$) is very similar to each other (Table 1). The structures of **TS2s** and **TS2g** are shown in Figure 6. The structures of **TS2s** and **TS2g** are similar to the

Scheme 3. Chemical Models of Reductive Elimination of the $(CH_3)_3M(III)$ Complexes (M = Cu, Ag, and Au)

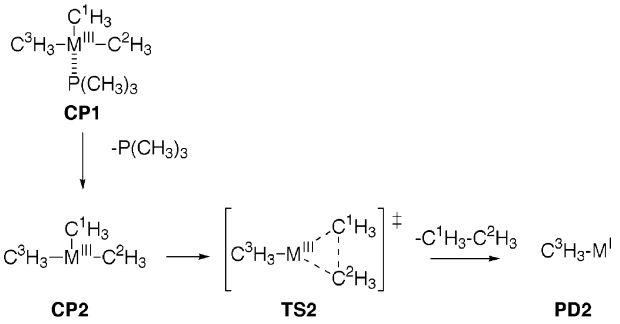

Table 1. Activation Energies for the Reductive Elimination of **CP1** ($\Delta E_1^{\ddagger}$), Taken from Figure 3a and for the Reductive Elimination of **CP1** via **CP2** ($\Delta E_2^{\ddagger}$)

M	$\Delta E1^{\ddagger}$ (kcal/mol)	$\Delta E2^{\ddagger}$ (kcal/mol)
Cu	17.7	
Ag	24.9	26.5
Au	35.0	37.1

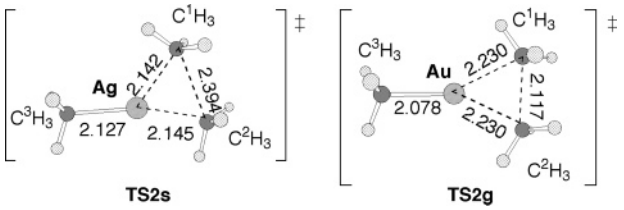

Figure 6. TSs of decomposition of $(CH_3)_3M(III)$ (M = Ag and Au) (**TS2**) at the B3LYP/631SDD level. Numbers refer to bond lengths (Å).

Scheme 4. Proposed Reaction Path of Alkylation of Alkyl Halide by Organogold Reagent

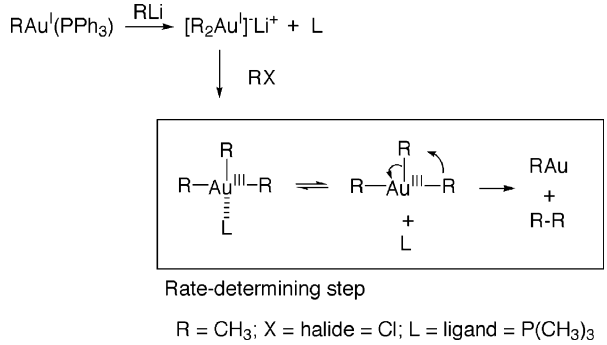

$(CH_3)_3M(III)$ moieties in **TS1s** and **TS1g**, respectively. The structures and energies suggest that **TS1** is essentially identical to **TS2** for silver and gold. The energetic and structural studies along the line shown in Schemes 2 and 3 therefore indicate that $(CH_3)_3Cu(III)\cdot P(CH_3)_3$ decomposes as it is, while the silver and the gold counterparts undergo dissociative decomposition through a Y-shaped TS such as **TS2s** and **TS2g**. This conclusion is consistent with the experimental results reported for a gold(III) complex (Scheme 4).[34]

Energetics Associated with Deformation of T-Shaped Intermediate toward TS. The copper(III) intermediate **CP1c** undergoes reductive elimination rather quickly with retention

(33) Reference deleted in proof.
(34) Komiya, S.; Kochi, J. K. *J. Am. Chem. Soc.* **1976**, *98*, 7599−7607. Komiya, S.; Albright, T. A.; Hoffmann, R.; Kochi, J. K. *J. Am. Chem. Soc.* **1976**, *98*, 7255−7265.

Table 2. Deformation Energies (DEF) and Interaction Energies (INT) for $(CH_3)_3M(III)\cdot P(CH_3)_3$ (M = Cu, Ag, and Au) (**CP1** and **TS1**)[a]

	Cu	Ag	Au
INT_{CP}	−27.3	−27.6	−35.9
INT_{TS}	−10. 4	−1.8	−2.1
INT_{total}	16.9	25.8	33.8
DEF_{F1}	1.7	0.5	3.2
DEF_{F2}	−0.9	−1.4	−2.0
DEF_{total}	0.8	−0.9	1.2
ΔE	17.7	24.9	35.0

[a] DEF and INT compose the activation energy ($\Delta E^{\ddagger}$). DEF_{F1} and DEF_{F2} are the DEF of $(CH_3)_3M(III)$ and $P(CH_3)_3$, respectively. $\Delta E^{\ddagger} = INT_{total} + DEF_{total}$; $DEF_{total} = DEF_{F1} + DEF_{F1}$; $INT_{total} = INT_{TS} - INT_{CP}$.

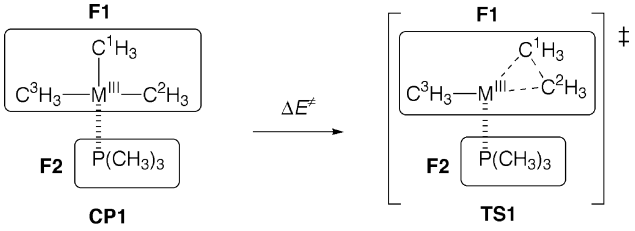

Figure 7. Reductive elimination of $(CH_3)_3M(III)\cdot P(CH_3)_3$ (M = Cu, Ag, and Au) for fragment energy analysis.

of the planar tetracoordinated geometry, while the gold(III) complex **CP1g** releases the phosphine ligand before reaching the TS of C−C bond formation. The latter is a rather high-energy process. The silver complex **CP1s** behaves in an intermediary manner (Figures 3 and 5). Fragment energy analysis[35] was performed to understand the origin of this difference (Table 2). In this analysis, $(CH_3)_3M(III)$ (**F1**) and $P(CH_3)_3$ (**F2**) in **CP1** and **TS2** are considered separately (Figure 7). The energy of **TS1** relative to the **CP1** ($\Delta E^{\ddagger}$) is formally divided into two parts, deformation energy (DEF_{total}) and interaction energy (INT_{total}) (Table 2). DEF_{total} is the sum of DEF_{F1} and DEF_{F2}; DEF_{F1} is the energy required to deform **F1** in **CP1** to that in **TS1**, and DEF_{F2} is the same energy for **F2**. INT_{total} is the sum of the gain of the interaction energies for **F1** and **F2** as the reaction goes from **CP1** to **TS1**.

In the initial coordination complexes (**CP1**), **F1** and **F2** interact most strongly in the gold complexes (**CP1g**; INT_{CP} = −35.9 kcal/mol), followed by the silver (**CP1s**; INT_{CP} = −27.6 kcal/mol) and the copper complexes (**CP1c**; INT_{CP} = −27.3 kcal/mol). The stronger interaction of **F1** and **F2** in the gold complex can be attributed to the high Lewis acidity of gold(III). In **TS1**, the interaction energies for the gold (INT_{TS} = −2.1 kcal/mol) and for the silver complex (INT_{TS} = −1.8 kcal/mol) are very small, while it is rather large (INT_{TS} = −10.4 kcal/mol) for copper. This coincides with the fact that the phosphine ligand dissociates from the silver and gold center in the **TS1** and therefore has no stabilizing effect in the transition state. The phosphine ligand, however, remains to be coordinated in **TS1** of copper and hence lowers the activation energy (Figure 5). The total deformation energies DEF_{total} are very small for all metals, since the deformation energy for each fragment, **F1** (DEF_{F1}) and **F2** (DEF_{F2}), is small for all metals ($DEF_{F1} + DEF_{F2} = DEF_{total}$, Cu: 0.8; Ag: −0.9; Au 1.2 kcal/mol). Consequently, the activation energy of the reaction ($\Delta E^{\ddagger} = INT_{total} + DEF_{total}$) largely depends on the interaction energy that is directly related

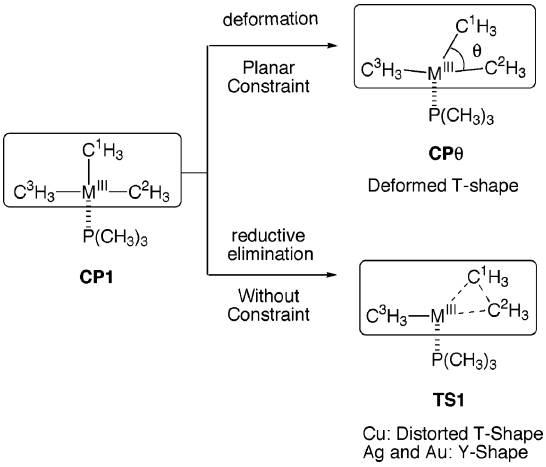

Figure 8. Chemical model for planar tetracoordinated TSs. The structure in box is the same as the one defined as **F1** in Figure 7.

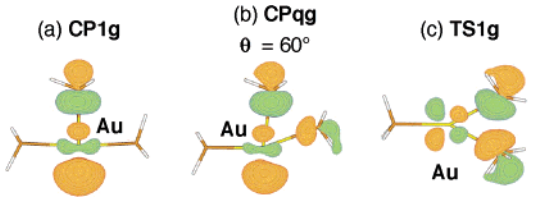

Figure 9. LUMO of the $(CH_3)_3Au(III)$ fragment in **CP1g** (a), **CP**θ**g** (θ = 60°) (b), and **TS1g** (c).

to the retention or the loss of the ligand coordination upon going from **CP1** to **TS1** (that is, the ligand loss in the Y-shaped TS for silver and gold accounts for the high activation energies).

To study the reason the ligand dissociates from silver and gold atoms in **TS1**, we deformed **CP1** by reducing the C^1-M-C^2 angle (θ) while forcing all heavy atoms to stay in a plane (**CP**θ) (Figure 8). The C^1-M-C^2 angle was decreased from 80 to 60°, and all other parts are optimized. Keeping strong interaction with the metal vacant orbital (Figure 9 shown for Au), the phosphine ligand does not dissociate from the central metals for all three cases (Figure 11), and the energy sharply increases for gold (+31.0 kcal/mol) and moderately for silver (+21.4 kcal/mol) and copper (+20.1 kcal/mol) at 60° (Figure 10a). These energy losses are comparable to the activation energies of reductive elimination of each complex (Figure 3a: Cu (+17.7 kcal/mol), Ag (+24.9 kcal/mol), Au (+35.0 kcal/mol); and Figure 5S: Ag (+26.5 kcal/mol), Au (+37.1 kcal/mol)).

When we focused on the $(CH_3)_3M(III)$ fragment (**F1**) in the phosphine complex, we obtained an energy diagram as Figure 10b, generally comparable to Figure 10a except for the copper at θ = 60°. The energy drops for copper because ethane starts to form at this geometry. The negative charge on the C^1H_3 group of **CP**θ (θ = 60°) in Figure 11 is −0.16 (i.e., closer to zero) making it ready to form a C−C bond with the neighboring C^2H_3 group. On the other hand, the charges in the silver and gold complexes are more negative (−0.18 and −0.23, respectively). Since the ligand is strongly coordinated to the silver or gold atom and increases the negative charge on the C^1H_3 group, removal of the phosphine ligand in the T-shaped complex is necessary here for the reductive elimination to occur.

Comparison between the Kohn−Sham orbitals of the T-shaped **CP**θ (θ = 60°) and **TS1** (Figure 12) illustrates the

(35) Nakamura, E.; Nakamura, M.; Miyachi, Y.; Koga, N.; Morokuma, K. *J. Am. Chem. Soc.* **1993**, *115*, 99−106.

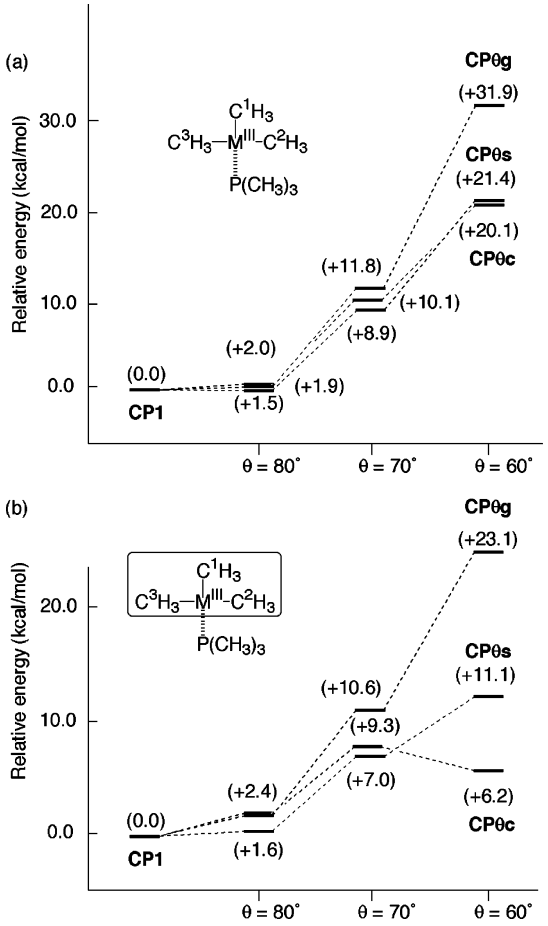

Figure 10. Relative potential energy of (a) deformed $(CH_3)_3M(III)\cdot P(CH_3)_3$ (M = Cu, Ag, and Au) (**CP**θ) and (b) their $(CH_3)M(III)$ moiety (**F1**) only (M = Cu, Ag, and Au).

similarity and the difference of orbital requirements among copper, silver, and gold in the reductive elimination. A Kohn−Sham orbital (HOMO-9) of the copper complex **CP**θ**c** (θ = 60°) (Figure 12a) shows an in-phase stabilizing interaction between the d_{z2} orbital of copper and the forming C^1-C^2 σ-bond (orange-colored orbital is about to form a bond). In the silver and gold, such a favorable interaction for new C−C bond forming does not exist. The d_{zx} orbitals of **CP**θ**s** (HOMO-1) and **CP**θ**g** (HOMO-1) have out-phase interaction with the forming C−C σ-bond. (For some other relevant orbitals of **CP**θ (θ = 60°) see Figure 9S in Supporting Information). On the other hand, the same orbital responsible for the C−C bond formation in the silver and gold complexes interacts with the metal d_{zx} orbital in an out-of-phase fashion, which destabilizes the process of the C^1-C^2 σ-bond formation. This is a reason that T-shaped TS is unfavorable for silver and gold.

The Kohn−Sham orbitals of **TS1** for the three metals (Figure 12b) give us similar information but a slightly different perspective. Not unexpectedly, the copper moiety of the T-shaped **CP**θ**c** (θ = 60°) and **TS1c** shows a similar orbital picture, but the Y-shaped TS of gold (**TS1g**) also shows similar in-phase interaction between the d_{z2} orbital of gold and the forming C^1-C^2 σ-bond. The situation with silver is intermediary. (For some other relevant orbitals of **TS2s** and **TS2g**, see Figure 9S in Supporting Information).

2.2. Reductive Elimination of π-Ally Diorganometal(III) $(CH_3)_2$(allyl)M(III). The π-allylmetal(III) model **CPa**, **Tsa**,

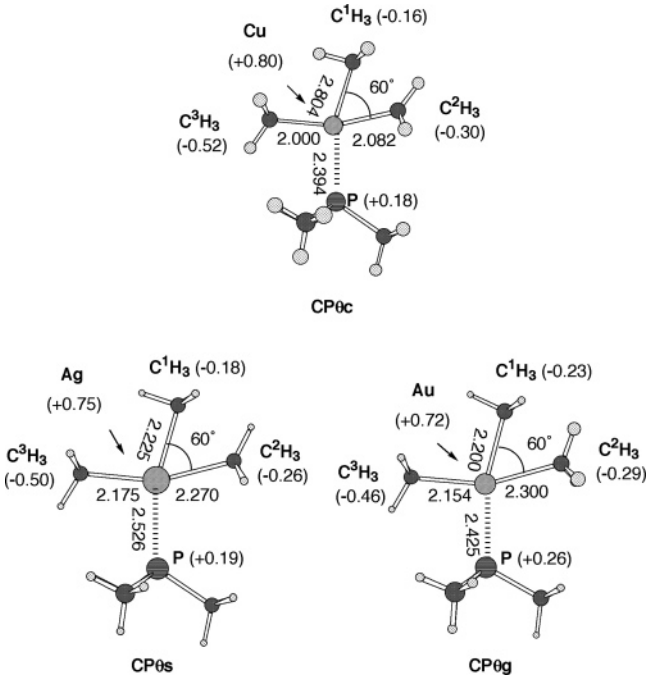

Figure 11. 3D structures of deformed $(CH_3)_3M(III)\cdot P(CH_3)_3$ (M = Cu, Ag, and Au) (**CP**θ) at the B3LYP/631SDD level. Numbers refer to bond lengths (Å). The natural charges are shown in parentheses.

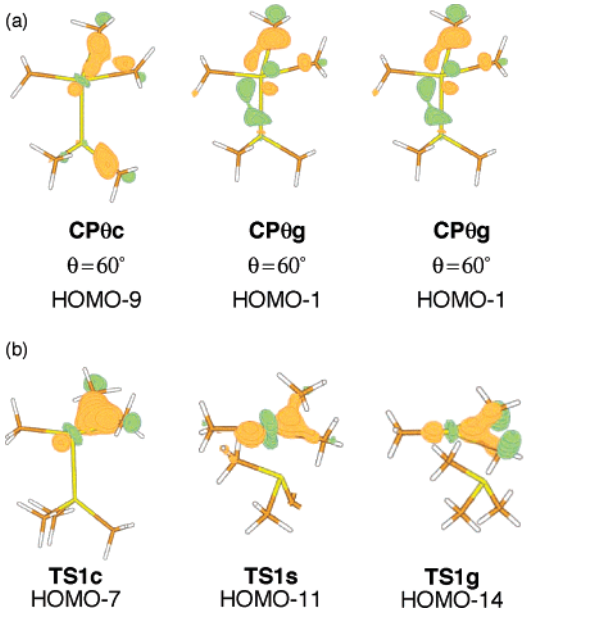

Figure 12. Kohn−Sham orbitals of (a) **CP**θ and (b) **TS1** potentially responsible for $^1C-^2C$ σ-bond formation.

and **PDa** can be viewed as an all-carbon analogue $(CH_3)_3M(III)\cdot P(CH_3)_3$ model since the C^1-C^2 double bond acts as a ligand to M(III) in place of phosphine ligand. This model provides a useful model to study the second half of the pathway of the conjugate addition of organocuprate(I) to α,β-unsaturated ketones (Figure 1).[5,18] The reaction of the copper series begins with the π-allyl dimethylmetal(III) (**CPa**) and goes through an enyl[$\sigma+\pi$] **TSa** to **PDa** (Scheme 5).[18] An alternative pathway through a σ-bonded allylcopper complex (to be discussed for Scheme 6) is a higher energy path.

Potential Energy Profiles of the Reaction Path. The energy profiles are shown in Figure 15. The activation potential

Scheme 5. Chemical Models of Reductive Elimination of π-Allyl Dimethylmetal(III) Complexes (M = Cu, Ag, and Au)

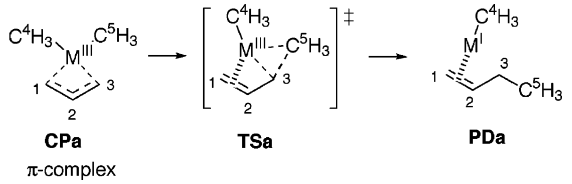

Scheme 6. Chemical Models of Reductive Elimination of σ-Allyl Dimethylmetal(III) Complexes (M = Cu, Ag, and Au)

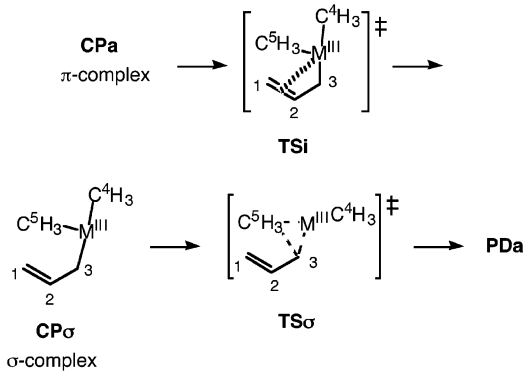

energy of the reductive elimination of $(CH_3)_2$(allyl)M(III) is +15.0 kcal/mol for copper, +17.8 kcal/mol for silver, and +23.2 kcal/mol for gold. As in the $(CH_3)_3M(III)\cdot P(CH_3)_3$ model, copper is kinetically the least stable.

The structures of the $(CH_3)_2$(allyl)M(III) complexes **CPa** are essentially the same as each other for all three metals (Figure 14), but those of the TSs (**TSa**) are not (Figure 15). In **TSac**, the π-allyl moiety is symmetrical (Cu−C^1: 2.214; Cu−C^3: 2.157), but, in **TSas** and **TSag**, it is unsymmetrical (Ag−C^1: 2.763; Ag−C^3: 2.338, Au−C^1: 3.107 Å; Au−C^3: 2.306 Å). The lateness of the latter TS must be related to the high activation energy of the reductive elimination.

The "T-shape" and "Y-shape" geometries discussed for $(CH_3)_3M(III)\cdot P(CH_3)_3$ are also found in the π-allyl case. One finds the T-geometry in **TSac** for the $C^5H_3/C^4H_3/C^3H_2$/Cu moiety and the Y-geometry in **TSag** for the same moiety. Particularly noteworthy is the entire loss of the coordination of the internal olefinic bond ($C^1H_2-C^2H_2$) to the gold metal in **TSag**.

The Kohn−Sham orbitals that describe π orbitals of C^1-C^2 in **TSa** are shown in Figure 16. In **TSac**, the olefin π-bond is donating electrons to the copper atom, but this effect is rather

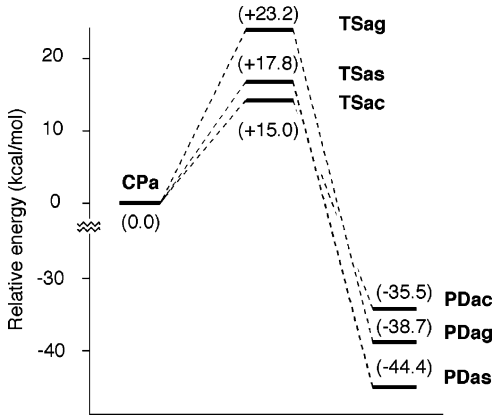

Figure 13. Potential energy profile of the reductive elimination of (CH_3)(allyl)M(III) (M = Cu, Ag, and Au) at the B3LYP/631SDD level.

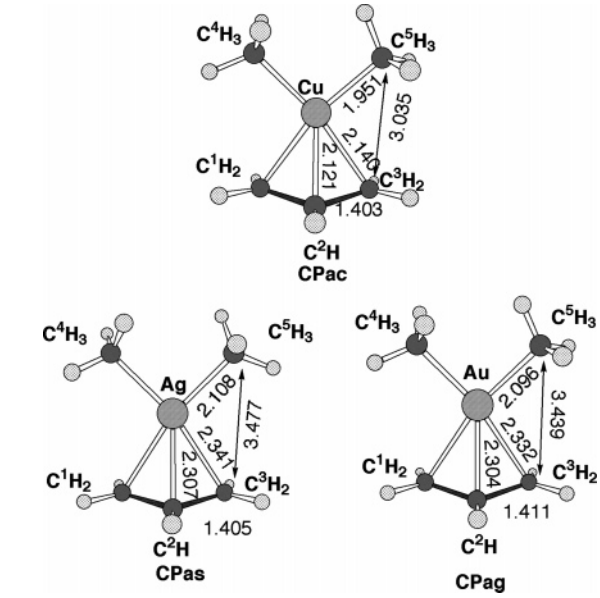

Figure 14. 3D structures of π-allyl dimethylmetal(III) complexes (**CPa**) at the B3LYP/631SDD level. Numbers refer to bond lengths (Å).

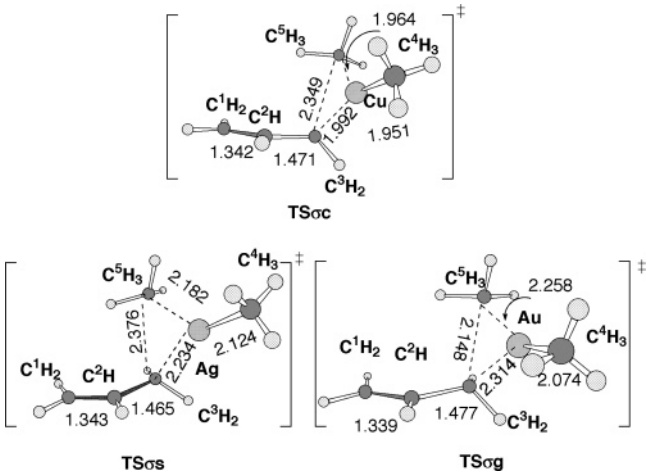

Figure 15. TSs of π-allyl dimethylmetal(III) complexes (**TSa**) at the B3LYP/631SDD level. Numbers refer to bond lengths (Å).

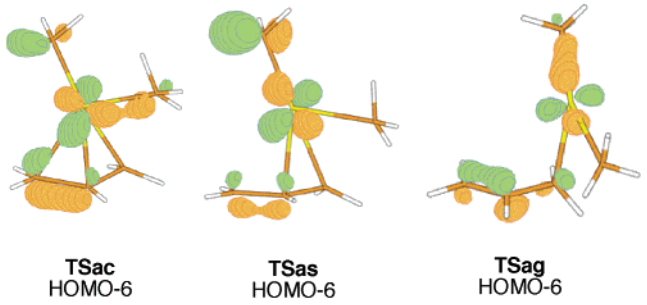

Figure 16. Kohn−Sham orbitals of TSs of the reductive elimination of π-allyl complex (**TSa**).

small in the silver case **TSas**. In the gold complex **TSag**, there is no donative coordination from the olefin to the gold metal.

In the reductive elimination of the π-allylcopper complex, we have already shown[18] that it can take place via a high-energy pathway involving the σ-complex **CP**σ and the σ-allylic TS (**TS**σ) (Scheme 6). This pathway is also available for the silver and the gold complexes, and their energetics are shown in Table 3. Unlike the copper complex in the first row, the σ-pathway in the

Table 3. Activation Energies for the Reductive Elimination of π-Complex (**CPa**) ($\Delta E_a^{\ddagger}$), Taken from Figure 13, and for the Reductive Elimination of the σ-Complex(**CP**σ) via **TS**σ ($\Delta E_b^{\ddagger}$)

M	$\Delta E_a^{\ddagger}$ (kcal/mol)	$\Delta E_b^{\ddagger}$ (kcal/mol)
Cu	15.0	18.4
Ag	17.8	18.8
Au	23.1	22.4

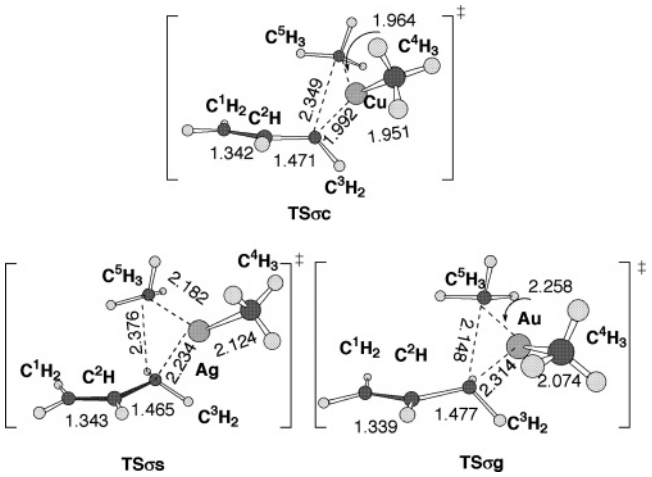

Figure 17. TSs of σ-allyl dimethylmetal(III) complexes (**TS**σ) at the B3LYP/631SDD level. Numbers refer to bond lengths (Å).

silver and the gold complexes is energetically comparable to the π-pathway shown in Figure 13. Indeed, the TSs of silver and gold complexes for the σ-path (Figure 17, **TS**σ**s** and **TS**σ**g**) are mere conformational isomers of the **TSas** and **TSag** (Figure 15).

Conclusion

The desire to understand the similarity and the difference among elements is a fundamental motivation of chemical research. In the present article, we have discussed the origin of the high nucleophilic reactivities of organocuprate(I) compounds as opposed to their lack for the corresponding silver and gold complexes on the basis of quantum mechanical calculations. The primary reason for the high reactivity of copper is the high-lying 3d-orbitals that can directly participate in the nucleophilic reactions, and the silver and gold ate complexes are unreactive because of the low-lying 4d and 5d orbitals, respectively. This effect of the orbital arises because the 4d and 5d metal orbitals are lower in energy than the 3d orbitals, since d−d repulsions are smaller for the diffuse 4d and 5d orbitals than for the contracted 3d orbitals, and this difference should increase from the early to the late transition metals.[36] Because of the relativistic effect, the energies of 4d and 5d metal orbitals are rather close to each other.[37,38]

Even though the starting ate complex $R_2M(I)^-$ may be reactive enough in practice, it would be useless if the higher valence intermediate $R_2(E)M(III)$ is stable and does not readily decompose. It was found to be the case with silver and gold. The $R_3Ag(III)$ and $R_3Au(III)$ type intermediates decompose less readily than the Cu(III) compound. The higher stability of the gold intermediate must be in part the result of the higher stability of the carbon−gold bond than the carbon−copper bond,[12,39] which is due to the relativistic effect of gold.[37,40] Installation of an electron-withdrawing ligand on the gold(III) atom would be useful to destabilize the intermediate, and it should be installed in place of the methyl groups rather than the phosphine ligand since the latter would not be attached to the metal center anymore in the TS.

The reductive elimination of the $R_3Cu(III)\cdot L$ compound takes place with retention of the ligand L that may be either neutral or anionic, or bound either inter- or intramolecularly to the copper atom. We have shown in this study and in the previous studies that the nature of this ligand is a crucial factor that determines the kinetic and thermodynamic stability of the copper(III) intermediates and hence the reaction rate of the nucleophilic organocopper reactions. On the other hand, the reductive elimination of the $R_3Au(III)$ intermediate occurs with dissociation of the ligand in the transition state. Such a dissociative mechanism was proposed already in the 70s on the basis of experiments by Kochi and Komiya for the reductive elimination of $(CH_3)_3Au(III)\cdot PPh_3$,[34] and we now show that the transition-state geometry is Y-shaped as has been intuitively expected. By forcing the ligand not to spontaneously eliminate through the geometrical constraint, we have shown that the basic ligand strongly stabilizes the higher-oxidation state of gold; hence, the removal of the ligand through the Y-deformation is essential for the gold(III) complex to undergo reductive elimination.

Organozincate reagents show nucleophilic reactivities similar to (but lower than) the organocuprate reagents. Despite this apparent similarity, their reaction mechanisms are different from each other since the zinc d-orbitals are too much low-lying and the alkyl group on the zinc atom acts as a nucleophile.[9] The organocopper, silver, and gold ate complexes have a similar set of orbitals, but the d-orbitals of organosilver and gold complexes are still a bit too low to make these complexes to be useful nucleophiles.

Acknowledgment. We thank N. Yoshikai for helpful discussions and the Ministry of Education, Culture, Sports, Science, and Technology for financial support (Grant-in-Aid for Scientific Research, Specially Promoted Research). W.N. thanks the JSPS (Japan Society for the Promotion of Science) for predoctoral fellowship. This work was supported by the 21st Century COE Program for Frontier in Fundamental Chemistry. Generous allotment of computer time from the Institute for Molecular Science is gratefully acknowledged.

Note Added after ASAP Publication. After this article was published ASAP on January 15, 2005, corrections were made in the last paragraph of the Conclusions. "Organoborate reagents", "boron d-orbitals", and "boron atoms" were changed to "Organozincate reagents", "zinc d-orbitals", and "zinc atoms", respectively. The corrected version was published ASAP on January 20, 2005.

Supporting Information Available: Energies and Cartesian coordinates of stationary points. This material is available free of charge via the Internet at http://pubs.acs.org.

JA045659+

(36) Gerloch, M.; Constable, E. C. *Transition Metal Chemistry*; VCH: Weinheim, Germany, 1994.
(37) Tai, H. C.; Krossing, I.; Seth, M.; Deubel, D. V. *Organometallics* **2004**, *23*, 2343−2349.
(38) Hakkinen, H.; Moseler, M.; Landman, U. *Phys. Rev. Lett.* **2002**, *89*, 033401-1−033401-4. Seth, M.; Cooke, F.; Schwerdtfeger, P.; Heully, J. L.; Pelissier, M. *J. Chem. Phys.* **1998**, *109*, 3935−3943. Hrusak, J.; Hertwig, R. H.; Schroder, D.; Schwerdtfeger, P.; Koch, W.; Schwarz, H. *Organometallics* **1995**, *14*, 1284−1291.
(39) Lupinetti, A. J.; Fau, S.; Frenking, G.; Strauss, S. H. *J. Phys. Chem. A* **1997**, *101*, 9551−9559. Antes, I.; Frenking, G. *Organometallics* **1995**, *14*, 4263−4268.
(40) Pyykko, P. *J. Am. Chem. Soc.* **1995**, *117*, 2067−2070.